HHS Public Access

Author manuscript

Circ Res. Author manuscript; available in PMC 2020 February 15.

Published in final edited form as:

Circ Res. 2019 February 15; 124(4): 539–552. doi:10.1161/CIRCRESAHA.118.314050.

Predicting Patient Response to the Antiarrhythmic Mexiletine Based on Genetic Variation: Personalized Medicine for Long QT Syndrome

Wandi Zhu[1], **Andrea Mazzanti**[2], **Taylor L. Voelker**[1], **Panpan Hou**[1], **Jonathan D. Moreno**[1,3], **Paweorn Angsutararux**[1], **Kristen M. Naegle**[1], **Silvia G. Priori**[2,4], and **Jonathan R. Silva**[1]

[1]Department of Biomedical Engineering, Washington University in St. Louis, St. Louis, MO

[2]Molecular Cardiology, IRCCS Salvatore Maugeri Foundation, Pavia, Italy

[3]Division of Cardiology, Department of Medicine, Washington University in St. Louis, Saint Louis, MO, USA

[4]Department of Molecular Medicine, University of Pavia, Pavia, Italy.

Abstract

Rationale: Mutations in the *SCN5A* gene, encoding the α subunit of the Nav1.5 channel, cause a life-threatening form of cardiac arrhythmia, Long QT Syndrome Type 3 (LQT3). Mexiletine, which is structurally related to the Na^+ channel-blocking anesthetic lidocaine, is used to treat LQT3 patients. However, the patient response is variable, depending on the genetic mutation in *SCN5A*.

Objective: The goal of this study is to understand the molecular basis of patients' variable responses and build a predictive statistical model that can be utilized to personalize mexiletine treatment based on patient's genetic variant.

Methods and Results: We monitored the cardiac Na^+ channel voltage-sensing domain (VSD) conformational dynamics simultaneously with other gating properties for the LQT3 variants. To systematically identify the relationship between mexiletine block and channel biophysical properties, we used a system-based statistical modeling approach to connect the multivariate properties to patient phenotype. We found that mexiletine altered the conformation of the Domain-III VSD (DIII-VSD), which is the same VSD that many tested LQT3 mutations affect. Analysis of 15 LQT3 variants showed a strong correlation between the activation of the DIII-VSD and the strength of the inhibition of the channel by mexiletine. Based on this improved molecular-level understanding, we generated a systems-based model based on a dataset of 32 LQT3 patients,

Address correspondence to: Dr. Jonathan R. Silva, One Brookings Drive, Whitaker Hall, Room 290G, Saint Louis, MO, 63130, United States of America, Tel: 314-935-8837, jonsilva@wustl.edu.

This manuscript was sent to Jose Jalife, Consulting Editor, for review by expert referees, editorial decision, and final disposition.

In November 2018, the average time from submission to first decision for all original research papers submitted to *Circulation Research* was 12.76 days.

DISCLOSURES

None.

which then successfully predicted the response of 7 out of 8 patients to mexiletine in a blinded, retrospective trial.

Conclusions: Our results imply that the modulated receptor theory of local anesthetic action, which confines local anesthetic binding effects to the channel pore, should be revised to include drug interaction with the DIII-VSD. Using an algorithm that incorporates this mode of action, we can predict patient-specific responses to mexiletine, improving therapeutic decision making.

Subject Terms:

Arrhythmias; Basic Science Research; Electrophysiology; Ion Channels/Membrane Transport; Translational Studies

Keywords

Long QT syndrome; antiarrhythmic drug; ion channels; system biology; clinical trial; Na+ channel; mexiletine; precision medicine

INTRODUCTION

Class Ib antiarrhythmics are widely prescribed to treat patients with ventricular tachycardia, ventricular fibrillation[1], and Long QT (LQT) syndrome[2]. As a subset of the Class I agents that target the voltage-gated cardiac Na^+ channel $Na_V1.5$, Class Ib drugs preferentially inhibit the late component of the Na^+ current (I_{Na}). Consequently, these drugs shorten action potential duration (APD) and prolong the effective refractory period (ERP)[3], thereby reducing the risk of arrhythmia. Despite Class I agents' common clinical use, these drugs display high variability in efficacy and may cause a pro-arrhythmic response in some patients[2,4]. For example, the classic Cardiac Arrhythmia Suppression Trial (CAST) showed that patients treated with Na_V channel inhibitors encainide or flecainide (Class Ic) were 2-3 times more likely to experience adverse events than were patients prescribed a placebo[5]. This stunning clinical failure highlights our incomplete understanding of antiarrhythmic therapy and suggests that antiarrhythmic drug action is more complex than is currently reflected in the Vaughan-Williams classification scheme that is widely used in clinical practice today.

LQT syndrome is a life-threatening disorder that arises from the inability of the heart to properly repolarize leading to prolongation of the QT interval on an electrocardiogram. LQT type 3 (LQT3) syndrome is caused by mutations in the SCN5A gene that encodes Nav1.5. The main class of drugs, beta-adrenergic receptor antagonists or partial agonists (beta-blockers), used to treat LQT1 have limited effectiveness for LQT3 patients[6]. Consequently, LQT3 is difficult to clinically manage.

In recent clinical trials, the orally-available class Ib drug mexiletine effectively shortens QT interval in a subset of LQT3 patients[2]. Despite mexiletine's overall efficacy, a spectrum of QT shortening was observed in patients that carry different *SCN5A* variants, effects that were reflected in single-cell electrophysiology recordings[4]. A precise understanding of how

$Na_V1.5$ mutations alter sensitivity to mexiletine would enable prediction of patient-specific responses and the development of molecularly targeted therapies.

The Na_V channel is a multiprotein complex that contains the α-subunit, which is a monomer that forms the ion-conducting part of the channel. The alpha-subunit has four homologous domains (DI-DIV), each composed by six transmembrane segments, S1-S6[7]. S1-S4 of each domain form the voltage-sensing domain (VSD), and S5-S6 form the pore. Upon cell membrane depolarization, the VSDs activate, the pore opens, and Na^+ ions enter the cell. Replacing phenylalanine with lysine at position 1760 in the S6 segment of DIV (DIV-S6) in the Nav1.5 alpha-subunit eliminates UDB by lidocaine[8–10], suggesting that the drug binding site is within the pore region of this alpha-subunit.

Binding of local anesthetics to Nav1.5 also modulates the VSDs. The pore and VSDs are tightly coupled; therefore, conformational changes induced by the binding of drugs within the pore can affect the voltage and time dependence of VSD conformation. Experiments that monitor VSD activation show that, when lidocaine binds to the channel, it stabilizes an activated conformation of VSD of DIII (DIII-VSD)[11,12]. This phenomenon is thought to be caused by lidocaine holding the pore-forming S6 of DIII (DIII-S6) in a partially open conformation even under hyperpolarized potentials, which then allosterically modulates the DIII-VSD stabilizing the activated conformation[12].

We therefore hypothesized that the DIII-VSD contributes to the mechanism of mexiletine block of $Na_v1.5$ channels and the heterogenous response to mexiletine of different LQT3 variants. Using electrophysiological techniques to monitor channel gating properties and voltage-clamp fluorometry (VCF) to monitor VSD conformational dynamics, we found that the effects of mexiletine on $Na_v1.5$ channels depends on the DIII-VSD dynamics. From the analysis of channels with LQT3 variants, we generated a systems-based model that predicts patient response to mexiletine therapy based on channel molecular gating properties.

METHODS

Data availability.

The data that support the findings of this study are available from the corresponding author upon reasonable request.

Molecular biology.

cRNA for human Nav1.5 α subunit was produced from the pMAX vector. All mutagenesis was achieved using overlap extension PCR reaction, followed by In-fusion cloning (Clonetech). All mutations were confirmed with sequencing (Genewiz). Each plasmid was then linearized with PacI restriction enzyme. Capped mRNA was synthesized using the mMESSAGE mMACHINE T7 Transcription Kit (Life Technologies) and purified via phenol-chloroform extraction.

Voltage clamp fluorometry and patch clamp recording.

Four previously developed constructs for VCF were used in recordings (DI: V215C, DII: S805C, DIII: M1296C, and DIV: S1618C). mRNA of the $Na_V1.5$ channel constructs were

co-injected with the Na_V β1 subunit in *Xenopus* oocytes. Voltage clamp recordings were performed 4-5 days after injection. The recording set-up, solutions, and recording protocols for VCF are the same as described previously[13–15]. Mexiletine hydrochloride powder (Sigma) was dissolved in extracellular recording solution to a stock concentration of 4 mM. pH for the solution is adjusted to 7.4. Mexiletine was further diluted from the stock solution to various concentrations (2-2000 μM). During recordings, measurements were made from the same cell before and after addition of the indicated concentration of mexiletine. Mexiletine was manually perfused into the extracellular solution chamber in the cut-open voltage clamp set-up.

Human embryonic Kidney 293T (HEK 293T) cells, obtained from the American Tissue Culture Collection (Manassas, VA), were maintained in Dulbecco's Modified Eagle's Medium (DMEM, Gibco) supplemented with 10% FBS and 100U/ml Penicillin-Streptomycin, in 37°C, 5% CO_2 incubator. Cells from passage 30-32 were co-transfected with $Na_V1.5$ variant and β1 subunit with jetPRIME reagents (Polyplus). Patch clamp recordings were conducted 24-48h after transfection. Solutions and protocols used were the same as described previously[15].

Electrophysiology data analysis.

Data analyses were performed with Clampfit (v10; Molecular Devices), MATLAB (R2012a; MATLAB), and Excel (Microsoft). G-V, fluorescence-voltage (F-V), and SSI curves were quantified by fitting a Boltzmann function: $y = 1 / (1 + \exp((V - V_{\frac{1}{2}}) / k)$. DIII-VSD deactivation rate was quantified based on the time to 50% decay. Channel recovery from inactivation was fitted with a sum of exponents function: $y = C - Af * \exp\left(-\frac{t}{\tau f}\right) - As * \exp(-\frac{t}{\tau s})$, which accounts for both fast and slower components of recovery[17]. The $V_{1/2}$ of WT DIII F-V curves from 21 cells were tested with the One-sample Kolmogorov-Smirnov test. The test implies that the $V_{1/2}$ values are normally distributed. Thus, comparison of $V_{1/2}$ values of F-V curves between conditions or constructs were performed using paired or independent Student t test, respectively (Microsoft Excel). Comparisons of % of mexiletine block were performed with the non-parametric Mann–Whitney U test. The error bars shown in the figures represent the standard errors of mean (SEM). The number of trials (n) reported in figure legends represent biological replicates for each experimental condition.

Partial least-squares regression.

Channel parameters (predictor variables) and channel responses to mexiletine (response variables) were standardized using z-score transformation. Partial least-square (PLS) regression was performed using MATLAB function "plsregress". Model stability was examined with leave-one-out cross validation. Each perturbation (channel variant) is individually removed from the dataset, and a PLS regression model is built on the rest of the variants. Using this model, mexiletine responses are predicted for the removed variant and compared with the measured responses. The model's general ability to predict left-out data was measured by calculating the Q-squared (Q^2) values, which is the sum of squares of the

difference between predicted and real values, normalized by the total variability in data. Variable importance in the projection (VIP) scores for each gating parameter is ranked by its impact on model fitness (Q^2). One gating parameter is removed at a time, and cross-validated model fitness Q^2 is calculated for the model based on the rest of parameters. The lower the Q^2 is, the higher VIP score the gating parameter has.

Blind retrospective clinical trial.

Patients included in the study were referred to the Molecular Cardiology Division at ICS Maugeri Hospital in Pavia, Italy Patients were genotyped and identified as carriers of a DNA variant in the coding sequence of the SCN5A gene and they were treated with mexiletine. Demographic data, personal and family clinical history and follow up data were stored in a customized database. The study was approved by the ethics committee of the Institution[2].

All predictions were made without prior knowledge of clinical outcomes. Predictions were made based on patient QT_c baseline and their genetic variants. After measuring mutant channel gating properties, parameters were inputted into the mexiletine QT_c shortening PLS regression model, which then predicted post-mexiletine QT_c intervals. The predicted values were then compared to clinical data.

RESULTS

Mexiletine stabilizes the active conformation of the DIII-VSD.

We examined the effect of mexiletine on heterologously expressed Nav1.5 channels. The response to mexiletine was similar for some properties and different for others of the Class Ib antiarrhythmics. Like other Class Ib antiarrhythmics[16], mexiletine preferentially inhibited the late component of the Na^+ current (I_{Na}) compared with the effect on the peak current[16] (Fig 1A, top). Mexiletine also exhibited UDB (Fig 1A, bottom), which is a property of Class Ib antiarrhythmics that is reflected by an increase in the inhibitory effect as the channels are repetitively activated by depolarizing voltage pulses.

Binding of Class Ib drug lidocaine to the channel results in stabilization of the inactivated state, which is often reflected by a hyperpolarizing shift in the steady state inactivation (SSI) curve[8]. In contrast to lidocaine, mexiletine caused a minimal shift of the SSI curve (Fig 1B). However, similar to lidocaine, mexiletine delayed recovery from inactivation, especially the slow component of recovery (Fig 1C). Thus, mexiletine appeared to influence the inactivated state through a mechanism different from that of lidocaine.

Previously, multiple studies demonstrated that lidocaine block of Na_V channels enhances the stability of the DIII-VSD activated conformation[11,12]. Here, we tested mexiletine interaction with the Nav1.5 VSDs by voltage-clamp fluorometry (VCF)[15]. In these experiments, a fluorophore is tethered to the charged S4 segment of one of the four VSDs. As the VSD changes conformation, the environment around the fluorophore is altered, which changes emission from the fluorophore, enabling measurement of the time and voltage dependence of the VSD conformation[14]. The steady-state fluorescence voltage (F-V) curves represent the voltage-dependence of the VSD activated conformation. Among four domains, only the DIII F-V curve displayed a large hyperpolarizing shift ($\Delta V_{1/2} = -32.5 \pm 7.5$ mV, $p = 0.04$)

after mexiletine block (Fig 1D), implying that the DIII-VSD remains in an activated conformation at more negative potentials upon mexiletine binding. Comparing the fluorescence traces before and after mexiletine block showed that both DIII and DIV-VSDs have slower activation and deactivation kinetics in the presence of mexiletine (Fig 1D). Because the DIII and DIV-VSDs are tightly coupled[17], the mexiletine-induced alteration of the DIV-VSD kinetics may be a consequence of its effects on the DIII-VSD.

To account for mexiletine's effects on the DIII-VSD, we proposed a model for its mechanism of action. Binding of mexiletine within the channel pore prevents the DIII-pore domain (S5-S6) from transitioning to a completely closed conformation during membrane repolarization (Fig 1E). The partially open conformation of the DIII-pore causes the DIII-VSD to remain in the activated conformation. This is like previously reported mechanisms of the interaction of lidocaine with Na_V channels[12].

LQT3 variants with different mexiletine sensitivities have distinct voltage dependence of DIII-VSD activation.

To understand the molecular mechanisms underlying differences in mexiletine sensitivity among LQT variants, we tested channels with single point mutations R1626P or M1652R (Fig 2A), which exhibit different responses to mexiletine[4]. These two variants exhibited different responses to mexiletine under nonstimulated conditions, tonic block (TB), and under stimulated conditions, use-dependent block (UDB). Consistent with the previous studies, when compared to the effect of mexiletine on WT channels, the drug exerted TB of R1626P at lower concentrations (EC_{50} = 211 μM) and required higher concentrations to exert TB of M1652R (EC_{50} = 2035 μM). Mexiletine had an EC_{50}=761 μM for TB of WT channels (Fig 2B).

We assessed UDB by applying 400 ms depolarizing pulses at 2 Hz, mimicking conditions during ventricular tachycardia[4]. We found that WT and R1626P have comparable UDB (WT: EC_{50}=58 μM, R1626P: EC_{50}=57 μM), while M1652R has much lower UDB (EC_{50}=193 μM) (Fig 2C). We tested the UDB of mexiletine using the cut-open voltage clamp. The EC_{50} values that we observed with this method are higher than those reported using patch clamp analysis of HEK 293 cells[4]. We hypothesized that this difference is due to limited solution access to the cell membrane in the cut-open voltage clamp set-up during perfusion. To test this hypothesis, we measured dose responses using two-electrode voltage clamp (TEVC), which allows better access to the solution. TEVC recordings showed mexiletine EC_{50} values for each variant that were similar to previously reported values (Online Table I, Online Fig I), suggesting that, in the cut-open set-up, amount of mexiletine at the channel is approximately 3-fold lower than the perfused concentration (Online Table I). With this information, we can account for the differences in EC_{50} values that relate to methodology.

To probe the link between the DIII-VSD conformation and mexiletine block, we assessed the correlation between DIII-VSD conformation and sensitivity of the channel to mexiletine. We hypothesized that, if mexiletine block of the pore caused the DIII-VSD to remain in the activated position, then channels with an activated DIII-VSD conformation would facilitate mexiletine accessibility to the pore. VCF experiments showed that both mutations

significantly affected DIII-VSD conformation (Fig 2D, 2F), despite their locations in DIV-VSD, which is distant from DIII-VSD (Fig 2A). Compared to WT channels, the mexiletine-sensitive[4] R1626P mutant exhibited a hyperpolarized DIII F-V curve ($\Delta V_{1/2}$ = −38.9 mV, p = 0.02), suggesting that more DIII-VSDs were in an activated conformation at the resting membrane potential. Conversely, the mexiletine-insensitive[4] variant M1652R exhibited a depolarizing shift in the DIII F-V curve ($\Delta V_{1/2}$ = 28.2, p = 0.01), indicating that more DIII-VSDs were in deactivated conformation. The shifts in voltage dependence of the DIII-VSD activation mirrored the differences in block by mexiletine: The mutant with DIII-VSD in an activated conformation (R1626P) at the resting potential displayed higher TB. These results support our hypothesis of a reciprocal relationship between mexiletine block and DIII-VSD conformation of the mutants.

Conventionally, occupancy of the inactivated state has been considered the primary determinant of Class Ib drug action. Consequently, the modulated receptor model describes preferential drug binding to channels that are inactivated. To test this notion, we measured how variants affected the SSI curve. Although the most sensitive mutation R1626P shifted SSI prominently, the magnitude of the shifts by these two variants are not consistent with their differences in mexiletine block (Fig 2E).

To further test whether the conformation of DIII-VSD regulates mexiletine block independent of inactivation, we assessed TB of WT channels at various potentials ranging from −120 to −90 mV. At these holding potentials the WT channels exhibited full conductance (none in the inactivated state) (Fig 2E) and showed a range of DIII-VSD conformations (Fig 2D). At four different holding potentials, −120, −110, −100, and −90 mV, the channel showed altered TB by mexiletine (Fig 2H). Moreover, the amount of TB had a linear relationship with the fraction of DIII-VSDs in the activated conformation at those potentials (Fig 2H). This result showed that the proportion of channels in the inactivated state is not the only factor that determines effectiveness of mexiletine block.

Based on our results, we proposed a model that explains the difference in mexiletine sensitivity between the two LQT variants (Fig 2G). At resting membrane potential, DIII-VSD of the sensitive variant R1626P tends to occupy the activated conformation. Because the activated conformation of DIII-VSD is coupled to conformation of the DIII-pore, the pore adopts a conformation that facilitates mexiletine accessibility. In contrast, fewer of the DIII-VSDs of the insensitive mutant M1652R are in the activated conformation at these potentials, causing the DIII-pore to remain in a conformation that prevents mexiletine from binding.

Voltage-dependent, not lipophilic, block accounts for differences in mexiletine response among LQT3 variants.

The F1760K mutation eliminates UDB by lidocaine and prevents lidocaine from affecting gating currents. Based on this binding site, Hanck *et al.* categorized lidocaine block into two components: a voltage-independent lipophilic block and a voltage-dependent block[9]. Lipophilic block is independent of the putative binding site F1760. We tested whether the difference in the EC_{50} for TB by mexiletine among the R1626P, M1652R, and WT channels

is due to lipophilic or voltage-dependent block by monitoring their responses to mexiletine in the background of F1760K mutation.

We assessed the response of F1760K channels to mexiletine. Both TB and UDB by mexiletine are greatly reduced for the F1760K channel. Using VCF, we found that mexiletine did not alter the conformation of DIII-VSD of the F1760K mutant channel (Online Fig II). We measured mexiletine-induced TB at 500 μM, a concentration at which the difference in TB among the channels was evident (Fig 2B), in WT, R1626P, and M1652R channels that also had the F1760K mutation. The TB achieved with 500 μM mexiletine in channels with F1760K were similar (Fig 2I). Although not significant, with the F1760K background, R1626P even became slightly less sensitive than WT and M1652R. Thus, the differences in the EC_{50} values for mexiletine among these LQT variants appeared due to voltage-dependent block rather than lipophilic block.

Decoupling the DIII-VSD from the pore eliminates differences in mexiletine blockade among LQT3 variants.

To further understand how the DIII-VSD affects mexiletine block, we utilized the A1326W mutation (Fig 3A), which decouples DIII-VSD from the pore[18]. In channels with A1326W, mexiletine no longer affects the conformation of DIII-VSD (Online Fig IIIA), demonstrating that a connection between the DIII-VSD and the pore is required to observe the mexiletine effect on DIII-VSD conformation. Our hypothesis is that R1626P and M1652R have distinct mexiletine sensitivities due to differences in the voltage dependence of DIII-VSD activation, consequently altering pore accessibility by mexiletine. From this hypothesis, we predict that channels in which the DIII-pore is decoupled from the DIII-VSD by A1326W will exhibit similar mexiletine block. Indeed, we observed that, upon the addition of A1326W, mexiletine caused similar TB and UDB for the R1626P, M1652R, and WT channels (Fig 3B, C).

In the presence of the A1326W mutation, the differences caused by R1626P or M1652R mutation in DIII-VSD activation and SSI are preserved (Fig 3D, E), suggesting that the A1326W mutation does not interfere with voltage-dependent DIII-VSD conformational changes. We proposed a model to explain the elimination of mexiletine sensitivity by the A1326W mutation in the two LQT3 variants (Fig 3F). Although R1626P stabilized and M1652R destabilized the activated conformation of DIII-VSD, the channel pore remains in the same conformation with the same mexiletine accessibility, because A1326W decoupled the DIII-pore from the DIII-VSD. These results indicated that the differences in mexiletine sensitivity of R1626P and M1652R are a consequence of the effects of the mutations on DIII-VSD activation, which are transmitted to the DIII-pore to increase accessibility to mexiletine. Thus, removing the coupling between the DIII-VSD and pore abolished the differences in mexiletine sensitivity.

Voltage dependence of DIII-VSD activation determines mexiletine-induced tonic block (TB).

By studying two LQT variants with extremely high or low mexiletine sensitivity, we showed that the voltage dependence of DIII-VSD activation strongly affects mexiletine block. We explored if this mechanism is generally applicable to common LQT3 variants. We first

investigated how DIII-VSD activation modulates TB by mexiletine. TB is usually assessed at negative potentials (−100 mV), a voltage at which most LQT variants have similar level of inactivation. DIII-VSD activation occurs at much lower voltage range than closed-state inactivation. Consequently, at −100 mV, the variability in the proportion of channels with DIII-VSD in the activated conformation is high among LQT3 variants. We measured the gating properties of WT and 15 LQT3 variant channels and the mexiletine TB of these channels. Most variants that we analyzed are found in patients who were previously treated with mexiletine[2]. Even though the LQT variants span the channel (Fig 4A), many of the variants exhibited altered DIII-VSD activation. We observed a strong correlation between the voltage dependence of DIII-VSD activation ($V_{1/2}$ of DIII F-V) and TB by (R^2=0.90, Fig 4B). Higher TB occurred for channels that had DIII-VSD activation at more negative potentials (Fig 4B). Instead of a linear relationship, we fitted the data to a Hill function, because we expected that TB will saturate at the ends of the curve. Intriguingly, we found that the minimum TB saturated at 15% block, suggesting that 15% of mexiletine-mediated TB is lipophilic block[12] (low affinity, voltage-independent block).

We also investigated the relationship between SSI and TB to test the classical theory that closed-state inactivation promotes Class Ib block. In contrast to DIII-VSD activation, closed-state inactivation ($V_{1/2}$ of SSI) did not correlate well with mexiletine TB (R^2=0.48, Fig 4C). These results further support the hypothesis that voltage dependence of DIII-VSD activation rather than that of closed-state inactivation determines mexiletine TB.

Partial least-square regression model predicts mexiletine use-dependent block and late I_{Na} block.

UDB and late I_{Na} block are critical features of Class Ib drugs. UDB enables the drug to block channels during periods of heightened channel activity, as in tachycardia. Late I_{Na} block describes a unique property of Class Ib drug that preferentially blocks the late over the peak component of I_{Na}, which shortens the action potential duration (APD), while minimally affects the AP upstroke or conduction. Unlike TB, which occurs at resting potentials at which channels undergo limited conformational changes, UDB and late I_{Na} block involve many complex gating transitions, including the activation of the other three VSDs, pore opening, pore closing, channel inactivation, and channel recovery from inactivation. Due to the complexity of the molecular movements that affect UDB and late I_{Na} block, using a single gating parameter, such as SSI or DIII-VSD activation, to predict them is insufficient (Online Fig IV). To address this challenge, we applied a data-driven modeling approach to identify the multivariate relationship between channel gating parameters and UDB or late I_{Na} block by mexiletine.

For each LQT variant, we quantified 14 gating parameters that describe gating processes, such as DIII-VSD, DIV-VSD activation, channel activation, and channel fast inactivation (Fig 5A). We also assessed UDB and late I_{Na} block by 250 μM mexiletine for each variant. To understand how these gating phenomena related to drug block, we utilized the partial least-square (PLS) regression approach. Gating parameters were used as predictive inputs, and the measured UDB or late I_{Na} block was used as an output for the PLS regression model. The PLS regression method has the ability to identify relationships between the

measured gating parameters and drug block and also reduce redundancy amongst the input parameters

We first applied feature selection among the 14 gating parameters to identify the most important parameters in determining mexiletine UDB or late I_{Na} block. Feature selection was based on the VIP (variable importance in projection) score of each parameter (See Materials and Methods), which describes parameter impact on model fitness. Gating parameters with high VIP scores (Fig 5A bottom, red squares) were then extracted to build the final PLS regression model for prediction. The VIP scores suggest that 5 gating parameters are crucial for determining UDB, including voltage dependence of channel conductance ($V_{1/2}$ of G-V), DIII-VSD activation ($V_{1/2}$ of DIII F-V), DIV-VSD activation ($V_{1/2}$ of DIV F-V), time constant of slow recovery from inactivation (slow recovery τ), and late I_{Na}. 4 gating parameters are important for predicting late I_{Na} block, including DIII-VSD activation ($V_{1/2}$ of DIII F-V), steady-state inactivation ($V_{1/2}$ of the SSI), slow recovery from inactivation (slow recovery τ) and late I_{Na}. By reducing the number of gating parameters used in the model, feature selection not only helps prevent overfitting but also improves our understanding of the relationship between channel gating processes and drug response.

To reduce data dimensionality, we also decreased the number of principal components to 3 for UDB and 2 for late I_{Na} block, because the reduced components were sufficient to explain over 90% variants in the data. With the selected features and reduced components, the PLS regression model predicts the UDB with a R-squared (R^2) of 0.9, suggesting the model fits the data well. We further validated the model with “leave one out” cross-validation, as described in Methods. The cross-validated PLS regression model predicts the UDB with a Q-squared (Q^2) of 0.7 (Fig 5B). The Q^2 value calculated from cross-validation measures the model’s ability to predict left-out data. A positive Q^2 indicates the model has predictive relevance[19]. Compared to the best prediction using a single gating parameter (DIII-VSD activation), which has a Q^2 of 0.3, the PLS regression approach improved the prediction accuracy.

Likewise, the PLS regression model for late I_{Na} block has a R^2 of 0.6 and Q^2 of 0.5 (Fig 5C), suggesting the amount of late I_{Na} block by mexiletine can also be predicted from channel gating parameters.

Predicting patients’ QT_C shortening by mexiletine from channel gating parameters with PLS regression model.

We also built a PLS regression model to predict mexiletine-induced corrected QT_c shortening (ΔQT_c) in patients with the LQT3 variants for which we measured channel gating parameters. We obtained QT_c interval data before and after mexiletine for 32 patients with 13 different genetic variants from a previously published study[6]. The data was used as training and validation dataset for the model. Although some patients also received beta blocker metoprolol along with mexiletine, a review of their records showed that QT_c is not significantly different between patients treated with beta block and mexiletine and those treated with only mexiletine[2]. The VIP scores for ΔQT_c showed that only two gating parameters are important for determining the ΔQT_c: DIII-VSD activation and τ of slow recovery from inactivation (Fig 5A bottom). With these two parameters as inputs, the PLS

regression model has a R-square (R^2) of 0.7, suggesting the model fit the training dataset well. To test the model prediction performance, we further cross-validated with leave-one out validation. The model predicted QT_c shortening in patients with a Q-square (Q^2) of 0.6 (Fig 5D), demonstrating that the model has strong predictive value. To further test whether electrophysiology data collected from mammalian cell lines can improve the model prediction accuracy, we also recorded I_{Na} from 13 variants and WT channels expressed in HEK 293T cells (Online Table III). Notably, the important gating parameters for each variant correlate well between the two expression systems (Online Fig V). Using the gating parameters quantified from HEK cell recordings, and DIII-VSD parameters from VCF recordings in Xenopus oocytes, we reconstructed the PLS regression model for ΔQTc (Online Fig VA). The model has a R^2 of 0.7 and a Q^2 of 0.6 (Online Fig VB), which are comparable to the model based on gating parameters quantified from Xenopus oocytes, suggesting that the data collected with the oocyte expression system were sufficient for building the PLS regression model for QT_c prediction.

Our results indicated that the clinical efficacy of mexiletine can be predicted from measurements of gating parameters of the $Na_V1.5$ variants, supporting the notion that in vitro testing may help predict a patient's specific response to mexiletine[4]. We extended this observation by building a precise model for predicting patient specific QT_c shortening by mexiletine based on detailed biophysical parameters. Notably, LQT3 is usually inherited in an autosomal dominant manner, suggesting that the patients have heterogenous population of WT and LQT3-linked $Na_V1.5$ channels. As mexiletine preferentially inhibits late I_{Na} and channels with more activated DIII-VSD, its effects on the WT channels are relatively weak compared to LQT3-linked channels. Although the model only focuses on the LQT3-linked channels, it should be sufficient to explain and predict the differences in QT_c shortening among patients.

To validate if the gating parameters selected based on the VIP scores improved the prediction accuracy (model fitness) of the PLS regression models, we evaluated 1000 models with randomly selected parameters (blue bars, Online Fig VI A, B, C). Among these models, those that contain most of the preselected parameters (more than 3 out of 5 for UDB, 3 out of 4 for late I_{Na} block and 1 out 2 for ΔQT_c) had overall improved prediction accuracy, implying that VIP score is an effective method to rank gating parameter importance.

Test QTc shortening PLS regression model performance with a blind clinical trial.

To test the performance of the PLS regression model in predicting a set of new variants in a blinded setting, we conducted a blind retrospective clinical trial that involved 8 LQT3 patients carrying 5 distinct SCN5A variants (Table 1, Figure 6), which were not variants included in the training/cross-validation dataset. The 8 patients were previously treated with mexiletine and their electrocardiograms were recorded before and after treatment. Evaluators were blinded from these clinical data during prediction. We expressed the $Na_V1.5$ channel variants from those patients and tested them in vitro to obtain the two essential electrophysiological parameters for the prediction: DIII-VSD activation and slow recovery τ. We generated the predicted post-mexiletine QT_c is with the mexiletine QT_c shortening PLS

regression model, with an upper and lower bound based on the 95% confidence interval calculated from the cross-validated model.

Strikingly, 7 out 8 patients had post-mexiletine QT_c that aligned with our predictions (Table 1, Figure 6). We noted that the one outlier (N1774D) patient that we failed to predict had a baseline QTc of 814 ms, which is higher than most of the training data. Assembling patient data from both training and trial datasets, we observed a trend that patients with very high QTc baselines (> 650 ms) tend to have higher percentage of QT_c shortening by mexiletine, independent of their genetic variants (Online Fig VII). As a result, our current model is not suitable for predicting patients with very high baseline QT_c (> 650 ms). From this blind clinical trial, we validated that our PLS model accurately predicted patients' response to mexiletine therapy for those patients with a baseline lower than 650 ms.

DISCUSSION

Mexiletine, as an oral Class Ib agent, is prescribed to patients suffering from ventricular tachycardia (VT) and with a predisposition to sudden cardiac death, but who have a suboptimal response to β-blockers and the multitargeted antiarrhythmic amiodarone. Studies have shown that the efficacy of mexiletine is patient specific. However, the reason behind the patient specificity is poorly understood, resulting an inability to predict drug outcomes for a given patient. A better understanding of Class Ib drug action is needed to develop a precision approach to management of ventricular tachycardia. A well-defined example of mexiletine's variable efficacy is the LQT3 syndrome, an inherited arrhythmia syndrome caused by mutations in the *SCN5A* gene. Unlike other LQT syndromes, LQT3 patients usually experience episodes of ventricular tachycardia during rest and bradycardia[4,16,20]. Mexiletine is an effective therapy in suppressing arrhythmia events in some of these patients[2]. However, patients carrying different SCN5A variants show varying QT interval shortening with mexiletine therapy, suggesting that the genetic variants perturb the channel in diverse ways to alter the mexiletine-channel interaction and thus drug efficacy.

In this study, we investigated the molecular mechanism of drug action by determining how $Na_V1.5$ mutations alter the sensitivity to mexiletine. We showed that DIII-VSD conformation is essential for determining mexiletine blockade. We propose a model where an activated DIII-VSD causes the channel pore to remain in a partially open conformation that promotes mexiletine TB. Among the 15 common LQT3 variants tested, many variants altered the DIII-VSD conformation, despite their distant locations to the DIII-VSD. We observed that mexiletine TB strongly correlated with the voltage dependence of DIII-VSD activation but not with SSI, which further suggests that the DIII-VSD conformation rather than closed state inactivation of the channel controls the sensitivity to mexiletine TB.

To predict patient-specific response to mexiletine, we used a systems biology approach, PLS regression. With data collected from 15 LQT3 variants and WT channels, we built a PLS model that accurately predicted mexiletine UDB, late I_{Na} block and patients' QT_c shortening from measured channel gating parameters. Two gating processes, DIII-VSD activation and slow recovery from inactivation, greatly influenced all predictions, suggesting that they are important in modulating the dynamic interactions of mexiletine with the channel.

An updated VSD-modulated receptor model describing Class Ib molecular drug action.

The modulated receptor theory proposed by Hille has been applied for 40 years to describe Class Ib drug interaction with Na_V channels[21]. This theory includes three basic and modulated channel states that illustrate drug interactions with the channel pore: closed, open, and inactivated. The modulated receptor theory emphasizes the primary role of the inactivation gate in promoting and stabilizing drug blockade. As more information regarding channel structure has become available, it is apparent that many conformational changes that are spread throughout the channel work together to cause channel gating. The four VSDs exhibit varied behavior during gating, and each is coupled to the channel pore. Thus, subtle changes in VSD dynamics can affect pore conformation and vice versa.

Previous studies showed that lidocaine binding to the pore affected DIII-VSD dynamics[11,12]. We demonstrated that LQT3 variants alter the voltage dependence of the DIII-VSD activation, and channels that populated an activated DIII-VSD conformation exhibit increased mexiletine block. To form a more complete understanding of channel and Class Ib drug interactions, we considered various components of the channel. Based on these results, we propose an updated VSD-modulated receptor model that describes how conformations of the DIII-VSD, the pore, and the inactivation gate alter Class Ib drug blockade. In this updated model, we included 5 states: CR (pore closed, DIII-VSD resting), CA (pore closed, DIII-VSD activated), OA (pore open, DIII-VSD activated), IA (pore inactivated, DIII-VSD activated), and IR (pore inactivated, DIII-VSD resting (Fig 7). Drugs can block the channel from each state, but with different binding and unbinding affinities. When channels are in the CR state, drugs have a low binding rate, because the hydrophilic pathway is unavailable. When the DIII-VSD activates, channels enter the CA state, in which drugs have much higher accessibility to the pore. Finally, in the channel open (OA) and inactivated (IA) states drugs exhibit very high binding rates. After membrane repolarization, channel recovery from inactivation has slower kinetics compare to the DIII-VSD deactivation[22], causing the channel to enter the IR state. Drugs have both low binding and unbinding rates when the channel occupies this state. When channels are in CR and IR states, only the hydrophobic pathway is accessible.

Mexiletine interacts with the channel differently than lidocaine.

Due to the structural similarity between lidocaine and mexiletine, patients with ventricular tachycardia that respond well to intravenous lidocaine are often prescribed mexiletine for long-term treatment. However, mexiletine fails to prevent arrhythmia in a large fraction (50%) of these patients[23], and even induces severe arrhythmia in some cases[24]. This clinical outcome suggests that mexiletine and lidocaine have distinct interactions with the channel that were not previously defined. Notably, mexiletine (pK_a 9.52) is mostly charged and hydrophilic, whereas lidocaine (pK_a 7.6) is partly uncharged and hydrophobic at physiological pH. Here, our results showed that the activated conformation of the DIII-VSD is required for hydrophilic, not hydrophobic, drug access to the channel pore. Many LQT3 variants stabilize the DIII-VSD in its activated position, promoting mexiletine block through the hydrophilic voltage-dependent pathway, which explains why mexiletine is effective in managing LQT3 syndrome. In contrast, for treating ventricular tachycardia patients with normal $Na_V1.5$ channels that do not have activated DIII-VSDs, mexiletine may be less

effective than lidocaine. These results suggest that response to lidocaine may not be a good predictor of the clinical response to mexiletine therapy.

A better understanding of the drug mechanism suggests a novel therapeutic strategy.

The most severe side effect of Class I drugs is proarrhythmia, which is potentially due to conduction slowing, as peak I_{Na} is inhibited[25]. The prediction of peak I_{Na} block from the PLS regression models can help to identify the sensitivity for each variant. If a certain variant is susceptible to peak I_{Na} block, the dose of mexiletine can be adjusted accordingly to avoid the proarrhythmic effects.

We demonstrated several LQT3 variants are insensitive to mexiletine due to the less activated DIII-VSD conformation of the channel. To rescue their insensitivity, a new therapeutic strategy that uses a combination of drugs can potentially be employed. A drug that promotes DIII-VSD activation can be used in combination with mexiletine to improve antiarrhythmic efficacy in the insensitive variants. Several combination therapies of Na^+ channel blockers have been tested in clinical settings[26,27]. For instance, an early study suggested that a combination of oral mexiletine and flecainide prevents recurrence of ventricular tachycardia in patients that are nonresponsive to monotherapy[27]. From the present study, one may conjecture that flecainide may improve mexiletine efficacy by promoting DIII-VSD activation. However, the mechanism of why certain combinations improve efficacy is not known. More work needs to be done to systematically evaluate how different combination therapies alter channel conformations and gating to improve drug outcomes. As induced pluripotent stem cell (iPSC) derived cardiomyocytes have emerged as useful model for studying LQT syndrome[28], in the future studies, it may be possible to validate the PLS regression model based therapy predictions in the LQT3 patient iPSC derived cardiomyocytes.

For more general ventricular arrhythmias other than LQT3 syndrome, mexiletine has been prescribed to patients with recurrent ventricular tachycardia post myocardial infarction and ischemic heart diseases that are resistant to other conventional antiarrhythmic agents in early clinical studies[29]. Although mexiletine effectively suppressed episodes of premature ventricular contraction (PVC), it induced adverse side effects in some patients resulting in them withdrawing from therapy[30]. Side effects included severe nausea and tremor. The incidence of side effects is dosage dependent. To reduce the side effects of mexiletine, the dose must be lowered while preserving its blocking efficiency. A combined antiarrhythmic therapy that promotes DIII-VSD activation could resolve this challenge. Moreover, the patient-specific responses can be attributed to disparity in expression of $Na_V1.5$ isoforms (polymorphisms) and accessory Na_V β subunits[31,32]. The impacts of common polymorphisms[33] and interacting proteins on Na_V channels' responses to mexiletine need to be explored in the future studies.

Understanding channel electrophysiology data with a systems biology approach.

Data-driven modeling is commonly applied in the field of systems biology, due to the large-scale nature of non-intuitive experimental data from biological assays, such as microarray and gene sequencing[34]. Although the scale of data from channel electrophysiology

recordings is much smaller, data-driven modeling can still be very useful, because ion channels themselves are complex systems, in which many parts of the channel work in concert to generate time- and voltage-dependent gating. Different voltage protocols can isolate different channel gating processes. Although effective, these voltage protocols are not ideal, because the properties they measure overlap. For example, an inactivation change can affect protocols that measure activation by shutting down channels before the channels open maximally[35]. Statistical tools that can reduce data dimensionality, such as principal component analysis and partial least square regression can reduce redundant information in data recorded with different voltage protocols.

In addition to dimensionality reduction, the methods that we applied in this study have the advantage of recognizing the multivariate relationships between input (independent) and output (dependent) variables. It rotates the input data to new optimal dimensions that maximize the covariance between input and output data. Thus, PLS regression models can be trained with existing data, and then used to predict output of new input data. In this study, we built PLS regression models that predict mexiletine response using channel gating parameters. Since other Class I drugs, such as lidocaine and flecainide, have distinct chemical properties that potentially result in distinct interactions with the channel, the PLS regression model we developed for mexiletine cannot be directly implemented to predict patients' responses to other drugs. However, the same methodology can be applied to predict other Class I drug responses. In the future, if a series of PLS regression models for common Class I drugs is established, this series could be used to predict a patient's response to available drugs. When a patient is identified with a new genetic variant, a patient's response to various drugs could be predicted with the established PLS regression models. Moreover, a systems biology approach has the advantage of testing the outcomes of a combination of scenarios[36]. Different drug prediction models can be combined to discover an optimal therapy for a certain patient.

Clinical perspective.

With our new findings of how channel gating dynamics determine mexiletine blockade, we built a PLS regression model that uses channel gating parameters to predict patient-specific response to mexiletine. In a blind clinical trial, we validated that the model accurately predicted the majority of patients' post-mexiletine QT_c. Our understanding of the mexiletine molecular mechanism can be applied to predict patient-specific response to mexiletine, which demonstrates a precision medicine approach in improving clinical management of LQT3 syndrome.

Study limitations.

To best differentiate the changes in TB, UDB, and late I_{Na} block among different LQT3 variants in the cut-open voltage clamp set-up, we tested with a mexiletine concentration (250μM) that is higher than the clinical dose (10-40μM). As a result, our measurements of mexiletine block may not represent physiological conditions.

Since LQT3 is a rare disease and only a fraction of patients were treated with mexiletine, we have limited patient data for training the predictive model. The model performance can be improved as more patient data are added. In future studies, we hope to conduct a multicenter trial, to increase the sample size. We also noticed that our model underestimated mexiletine effects for patient carrying N1774D variant in the clinical trial. Based on our observations, the model tends to underestimate mexiletine's effect for patients with very long baseline QT_c (> 650ms). However, it is important to consider that even though mexiletine reduces QT_c in these patients, they still have high-risk QT_c post therapy, suggesting it is necessary to apply mexiletine in conjunction with other therapies. The inaccuracy of prediction can also result from the fact that the model only accounts for Na_V channel variations, while many other complex clinical variables, such as drug metabolism, can also significantly impact patients' responses to mexiletine.

Moreover, although the model can predict patients' post-mexiletine QTc interval, it is only an indicator of the risk for arrhythmia events. There is no clear definition of a safe range, which should be taken into consideration when using the model for prediction. The model also only reflects results from this study. Thus, it should not replace the current clinical guidelines for LQT3 syndrome, until further validation with prospective trials.

Conclusions.

Mexiletine is widely used as an antiarrhythmic drug for patients with LQT3 syndrome and ventricular tachycardia. Patient-specific responses to mexiletine have been observed in clinical studies. However, the underlying mechanism is not well defined due to the lack of understanding of mexiletine's molecular interactions with the $Na_V1.5$ channel. We demonstrate that the conformation of the DIII-VSD of the $Na_V1.5$ channel is crucial for determining mexiletine blockade. Using biophysical data and a systems biology approach, we built a model that can predict LQT3 patient QT_c shortening with mexiletine therapy based on channel gating parameters. Our findings also suggest a new antiarrhythmic strategy of combination therapies that target molecular conformations of the channel to increase mexiletine efficacy.

Supplementary Material

Refer to Web version on PubMed Central for supplementary material.

ACKNOWLEDGEMENTS

We thank Dr. Jeanne Nerbonne, Dr. Jianmin Cui for sharing resources and many helpful discussions, Dr. Nancy Gough for help with editing.

SOURCES OF FUNDING

This work was supported by AHA Predoctoral Fellowship 15PRE25080073 (WZ) and NIH R01 HL136553 (JRS), NIH R01 HL126774 and AHA Postdoctoral Fellowship 18POST34030203 (PH), and Training Grant T32 HL007081 (JM).

Nonstandard Abbreviations and Acronyms:

VSD
voltage-sensing domain

VCF
voltage clamp fluorometry

LQT
long QT syndrome

TB
tonic block

UDB
use-dependent block

DI, DII, DIII and DIV
Domain I, II, III, and IV

PLS
partial least square

REFERENCES

1. Priori SG, Blomström-Lundqvist C, Mazzanti A. 2015 ESC Guidelines for the management of patients with ventricular arrhythmias and the prevention of sudden cardiac death. Eur Heart J [Internet]. 2015;8:746–837. Available from: http://www.ncbi.nlm.nih.gov/pubmed/16935866
2. Mazzanti A, Maragna R, Faragli A, Monteforte N, Bloise R, Memmi M, Novelli V, Baiardi P, Bagnardi V, Etheridge SP, Napolitano C, Priori SG. Gene-specific therapy with mexiletine reduces arrhythmic events in patients with long QT syndrome type 3. J Am Coll Cardiol. 2016;67:1053–1058. [PubMed: 26940925]
3. Zipes DP, Jalife J. Cardiac Electrophysiology: From Cell to Bedside: Sixth Edition. 2013.
4. Ruan Y, Liu N, Bloise R, Napolitano C, Priori SG. Gating properties of SCN5A mutations and the response to mexiletine in long-QT syndrome type 3 patients. Circulation. 2007;116:1137–1144. [PubMed: 17698727]
5. Echt DS, Liebson PR, Mitchell LB, Peters RW, Obias-Manno D, Barker AH, Arensberg D, Baker A, Friedman L, Greene HL, Huther ML, Richardson DW. Mortality and Morbidity in Patients Receiving Encainide, Flecainide, or Placebo. N Engl J Med [Internet]. 1991;324:781–788. Available from: http://www.nejm.org/doi/abs/10.1056/NEJM199103213241201
6. Shimizu W, Antzelevitch C. Differential effects of beta-adrenergic agonists and antagonist in LQT1, LQT2 and LQT3 models of the long QT syndrome. J Am Coll Cardiol. 2000;35:778–786. [PubMed: 10716483]
7. Gellens ME, George AL, Chen LQ, Chahine M, Horn R, Barchi RL, Kallen RG. Primary structure and functional expression of the human cardiac tetrodotoxin-insensitive voltage-dependent sodium channel. Proc Natl Acad Sci U S A. 1992;89:554–558. [PubMed: 1309946]
8. Ragsdale DS, McPhee JC, Scheuer T, Catterall WA. Common molecular determinants of local anesthetic, antiarrhythmic, and anticonvulsant block of voltage-gated Na+ channels. Proc Natl Acad Sci U S A [Internet]. 1996;93:9270–9275. Available from: http://www.ncbi.nlm.nih.gov/pubmed/8799190%5Cnhttp://www.pubmedcentral.nih.gov/articlerender.fcgi?artid=PMC38631

9. Hanck DA, Nikitina E, McNulty MM, Fozzard HA, Lipkind GM, Sheets MF. Using lidocaine and benzocaine to link sodium channel molecular conformations to state-dependent antiarrhythmic drug affinity. Circ Res. 2009;105:492–499. [PubMed: 19661462]
10. Ragsdale DS, McPhee JC, Scheuer T, Catterall WA. Molecular determinants of state-dependent block of Na+ channels by local anesthetics. Science [Internet]. 1994;265:1724–8. Available from: http://www.ncbi.nlm.nih.gov/pubmed/8085162
11. Sheets MF, Hanck DA. Molecular Action of Lidocaine on the Voltage Sensors of Sodium Channels. J Gen Physiol [Internet]. 2003;121:163–175. Available from: http://www.jgp.org/lookup/doi/10.1085/jgp.20028651
12. Arcisio-Miranda M, Muroi Y, Chowdhury S, Chanda B. Molecular mechanism of allosteric modification of voltage-dependent sodium channels by local anesthetics. J Gen Physiol [Internet]. 2010;136:541–554. Available from: http://www.jgp.org/lookup/doi/10.1085/jgp.201010438
13. Rudokas MW, Varga Z, Schubert AR, Asaro AB, Silva JR. The Xenopus Oocyte Cut-open Vaseline Gap Voltage-clamp Technique With Fluorometry. J Vis Exp. 2014;85:1–11.
14. Zhu W, Varga Z, Silva JR. Molecular motions that shape the cardiac action potential: Insights from voltage clamp fl uorometry. Prog Biophys Mol Biol [Internet]. 2016;1–15. Available from: 10.1016/j.pbiomolbio.2015.12.003
15. Varga Z, Zhu W, Schubert AR, Pardieck JL, Krumholz A, Hsu EJ, Zaydman M a., Cui J, Silva JR Direct Measurement of Cardiac Na^+ Channel Conformations Reveals Molecular Pathologies of Inherited Mutations. Circ Arrhythmia Electrophysiol [Internet]. 2015;CIRCEP.115.003155. Available from: http://circep.ahajournals.org/lookup/doi/10.1161/CIRCEP.115.003155
16. Wang DW, Yazawa K, Makita N, George AL, Bennett PB. Pharmacological targeting of long QT mutant sodium channels. J Clin Invest. 1997;99:1714–1720. [PubMed: 9120016]
17. Peters CH, Yu A, Zhu W, Silva JR, Ruben PC. Depolarization of the conductance-voltage relationship in the NaV1.5 mutant, E1784K, is due to altered fast inactivation. PLoS One. 2017;
18. Muroi Y, Arcisio-Miranda M, Chowdhury S, Chanda B. Molecular determinants of coupling between the domain III voltage-sensor and pore of a sodium channel. Nat Struct Mol Biol [Internet]. 2010;17:230–237. Available from: http://www.ncbi.nlm.nih.gov/pmc/articles/PMC2879147/%5Cnhttp://www.ncbi.nlm.nih.gov/pmc/articles/PMC2879147/pdf/nihms197276.pdf
19. Hair JFJ, Hult GTM, Ringle C, Sarstedt M. A Primer on Partial Least Squares Structural Equation Modeling (PLS-SEM). 2014.
20. Schwartz PJ, Priori SG, Spazzolini C, Moss AJ, Vincent GM, Napolitano C, Towbin JA, Denjoy I, Wilde A, Guicheney P, Zareba W, Breithardt G, Robinson JL, Keating MT, Schulze-Bahr E, Bloise R, Beggs AH, Brink P, Toivonen L, Timothy KW, Corfield V, Wattanasirichaigoon D, Corbett C, Haverkamp W, Lehmann MH, Schwartz K, Coumel P. Genotype-phenotype correlation in the long-QT syndrome: gene-specific triggers for life-threatening arrhythmias. Circulation [Internet]. 2001;103:89–95. Available from: http://www.ncbi.nlm.nih.gov/pubmed/11136691
21. Hille B Local anesthetics: hydrophilic and hydrophobic pathways for the drug-receptor reaction. J Gen Physiol [Internet]. 1977;69:497–515. Available from: http://www.pubmedcentral.nih.gov/articlerender.fcgi?artid=2215053&tool=pmcentrez&rendertype=abstract
22. Hsu EJ, Zhu W, Schubert AR, Voelker T, Varga Z, Silva JR. Regulation of Na+ channel inactivation by the DIII and DIV voltage-sensing domains. J Gen Physiol [Internet]. 2017;Available from: http://jgp.rupress.org/content/early/2017/02/22/jgp.201611678.abstract
23. Zehender M, Geibel A, Treese N, Hohnloser S, Meinertz T, Just H. Prediction of efficacy and tolerance of oral mexiletine by intravenous lidocaine application. Clin Pharmacol Ther. 1988;44.
24. Cocco G, Strozzi C, Chu D, Pansini R. Torsades de pointes as a manifestation of mexiletine toxicity. Am Heart J. 1980;100:878–880. [PubMed: 7446392]
25. Crawford, Michael H, DiMarco, John P , Paulus WJ Cardiology. Elsevier; 2010.
26. Duff HJ, Mitchell LB, Manyari D, Wyse DG. Mexiletine-quinidine combination: Electrophysiologic correlates of a favorable antiarrhythmic interaction in humans. J Am Coll Cardiol. 1987;10:1149–1156. [PubMed: 3668109]

27. Jordaens LJ, Tavernier R, Vanmeerhaeghe X, Robbens E, Clement DL. Combination of Flecainide and Mexiletine for the Treatment of Ventricular Tachyarrhythmias. Pacing Clin Electrophysiol. 1990;13:1127–1135. [PubMed: 1700388]

28. McKeithan WL, Savchenko A, Yu MS, Cerignoli F, Bruyneel AAN, Price JH, Colas AR, Miller EW, Cashman JR, Mercola M. An automated platform for assessment of congenital and drug-induced arrhythmia with hiPSC-derived cardiomyocytes. Front Physiol. 2017; 8:766. doi: 10.3389/fphys.2017.00766 [PubMed: 29075196]

29. Duff HJ, Roden D, Primm RK, Oates JA, Woosley RL. Mexiletine in the treatment of resistant ventricular arrhythmias: enhancement of efficacy and reduction of dose-related side effects by combination with quinidine. Circulation. 1983;67:1124–1128. [PubMed: 6831673]

30. Group IR. International mexiletine and placebo antiarrhythmic coronary trial: I. Report on arrhythmia and other findings. J Am Coll Cardiol. 1984;4:1148–1163. [PubMed: 6209318]

31. Yuan L, Koivumäki JT, Liang B, Lorentzen LG, Tang C, Andersen MN, Svendsen JH, Tfelt-Hansen J, Maleckar M, Schmitt N, Olesen MS, Jespersen T. Investigations of the Navβ1b sodium channel subunit in human ventricle; functional characterization of the H162P Brugada syndrome mutant. Am J Physiol Heart Circ Physiol [Internet]. 2014 [cited 2015 Jan 7];306:H1204–12. Available from: http://www.ncbi.nlm.nih.gov/pubmed/24561865

32. Zhu W, Voelker TL, Varga Z, Schubert AR, Nerbonne JM, Silva JR. Mechanisms of noncovalent β subunit regulation of NaV channel gating. J Gen Physiol [Internet]. 2017;Available from: http://jgp.rupress.org/content/early/2017/07/17/jgp.201711802.abstract

33. Makielski JC, Ye B, Valdivia CR, Pagel MD, Pu J, Tester DJ, Ackerman MJ. A ubiquitous splice variant and a common polymorphism affect heterologous expression of recombinant human SCN5A heart sodium channels. Circ Res. 2003; 93:821–828. doi: 10.1161/01.RES.0000096652.14509.96 [PubMed: 14500339]

34. Janes KA, Yaffe MB. Data-driven modelling of signal-transduction networks. Nat. Rev. Mol. Cell Biol. 2006;7:820–828. [PubMed: 17057752]

35. Mangold KE, Brumback BD, Angsutararux P, Voelker TL, Zhu W, Kang PW, Moreno JD, Silva JR. Mechanisms and models of cardiac sodium channel inactivation. Channels [Internet]. 2017;11:517–533. Available from: 10.1080/19336950.2017.1369637

36. Fitzgerald JB, Schoeberl B, Nielsen UB, Sorger PK. Systems biology and combination therapy in the quest for clinical efficacy. Nat. Chem. Biol. 2006;2:458–466. [PubMed: 16921358]

NOVELTY AND SIGNIFICANCE

What Is Known?

- Mexiletine is effective in suppressing arrhythmia in some Long QT syndrome 3 (LQT3) patients.
- Successful mexiletine treatment is dependent on patient genotype.

What New Information Does This Article Contribute?

- Mutation effects on the cardiac Na^+ channel ($Na_V1.5$) conformation predict whether mexiletine will shorten patient QTc interval.
- The DIII voltage sensing domain (DIII-VSD) of the cardiac Na^+ channel is the primary regulator of mexiletine efficacy.

LQT3 is a genetic disease that leads to deadly arrhythmias. It is caused by mutations within *SCN5A*, which encodes $Na_V1.5$. The $Na_V1.5$ channel blocking drug, mexiletine, was shown to be effective in treating patients with LQT3. However, patients carrying certain mutations are unresponsive to mexiletine therapy. To understand this genetic-based variation in clinical outcome, we characterized and compared $Na_V1.5$ channels carrying different LQT3 mutations and exhibit varying mexiletine sensitivity. We identified a key regulator, the DIII-VSD of $Na_V1.5$. For the LQT3 variants that favor the DIII-VSD in the active conformation, mexiletine blockade is enhanced. Using this mechanism and other in vitro electrophysiology measurements, we created a system-based model that predicts patient response to mexiletine based on the $Na_V1.5$ mutation they carry. We validated the model's predictive ability with a blind clinical trial, establishing an approach that may be used to personalize treatment for LQT3 patients. We demonstrate for the first time, a drug outcome prediction which combines cellular electrophysiology and computational systems biology that is readily extendable to the class I family of antiarrhythmic drugs.

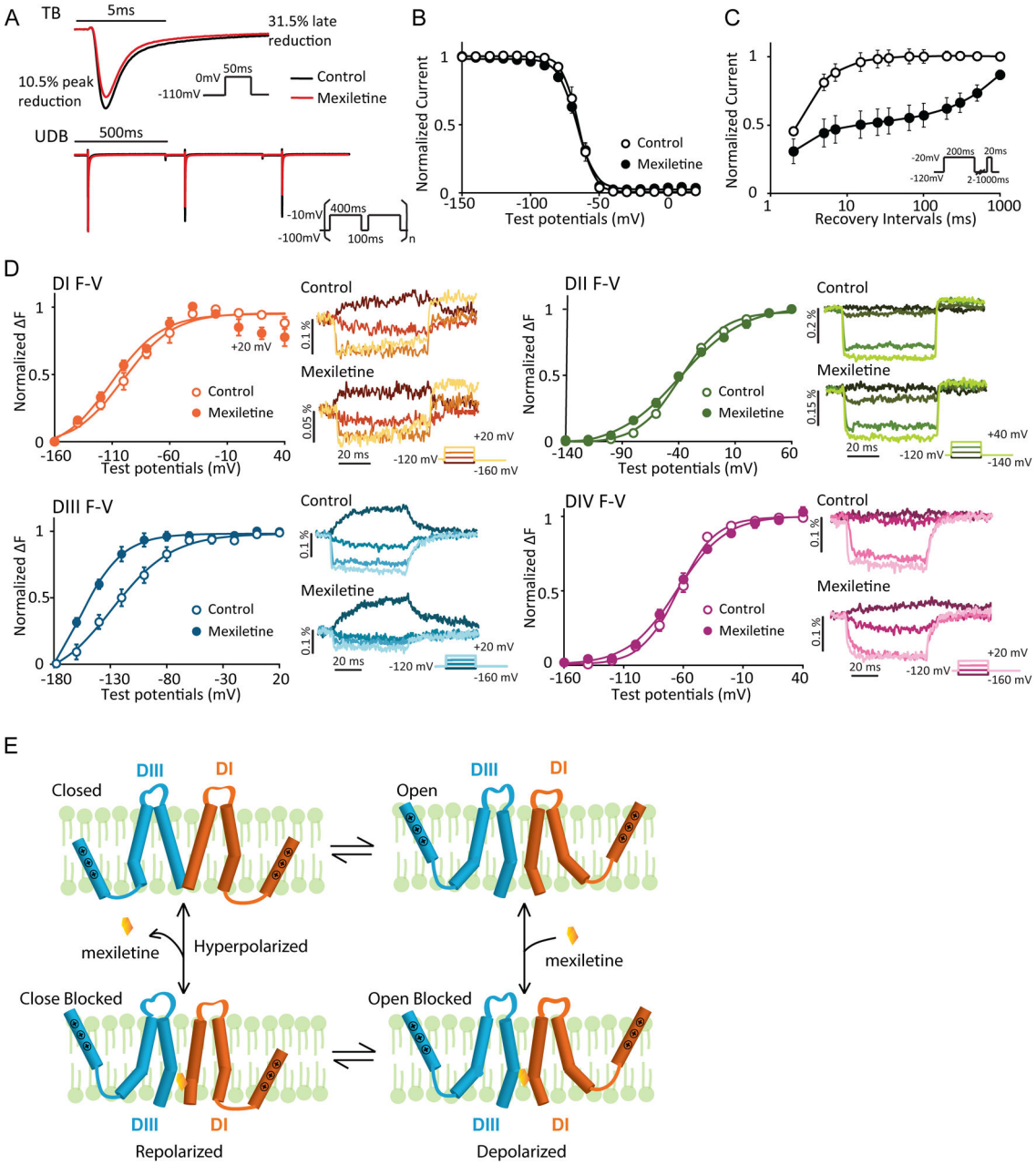

Figure 1: Mexiletine blockade of $Na_V1.5$ channel stabilize the DIII-VSD at the activated position.

A. Representative current traces before and after 250 μM mexiletine tonic block (TB) and use-dependent block (UDB). Comparison between traces before and after mexiletine shows that mexiletine reduces the peak current by 10.5%, but the later component (10ms after peak) by 31.5%. 250 μM mexiletine was used, because channels exhibit moderate TB and UDB at this concentration.

B. Steady-state inactivation (SSI) curves before and after 2 mM mexiletine (n=4). Channel SSI was tested by holding the cells from −150 to 20 mV with a 10-mV increment for 200 ms. Fraction of channels available were then measured by peak currents induced by a −20mV test pulse. Mexiletine induces minimal hyperpolarizing shift in SSI curve.

C. Channel recovery from inactivation curves before and after 250 μM mexiletine (n=3). Cells were first depolarized to −20 mV to induce inactivation, then allowed to recover at −120 mV for various durations. Fraction of channels recovered were then tested with a −20mV pulse. Mexiletine slows down both phases of recovery, especially the slow recovery.
D. Left panels: Voltage dependence of steady-state fluorescence (F-V curves) from four domains (DI-V215C, DII-S805C, DIII-M1296C, DIV-S1618C) before and after 4 mM mexiletine. The mean ± SEM is reported for groups of 4 to 8 cells. Fluorescence after mexiletine was measured after 80% tonic block. Right panels: representative fluorescence traces before and after mexiletine. Four voltage steps ranging from −160 to 20mV (DI, DIII, and DIV) or −140 to 40mV (DII) at a 40mV interval are shown. Mexiletine only affects DIII-VSD by causing a hyperpolarizing shift in DIII F-V curve and slows down DIII-VSD deactivation, without affecting other three domains.
E. Proposed schematic (adapted from Arcisio-Miranda lidocaine model[31]) showing the mechanism of mexiletine stabilization of activated DIII-VSD. Only DI and DIII are shown and the VSDs are represented by a single S4 segment for clarity.

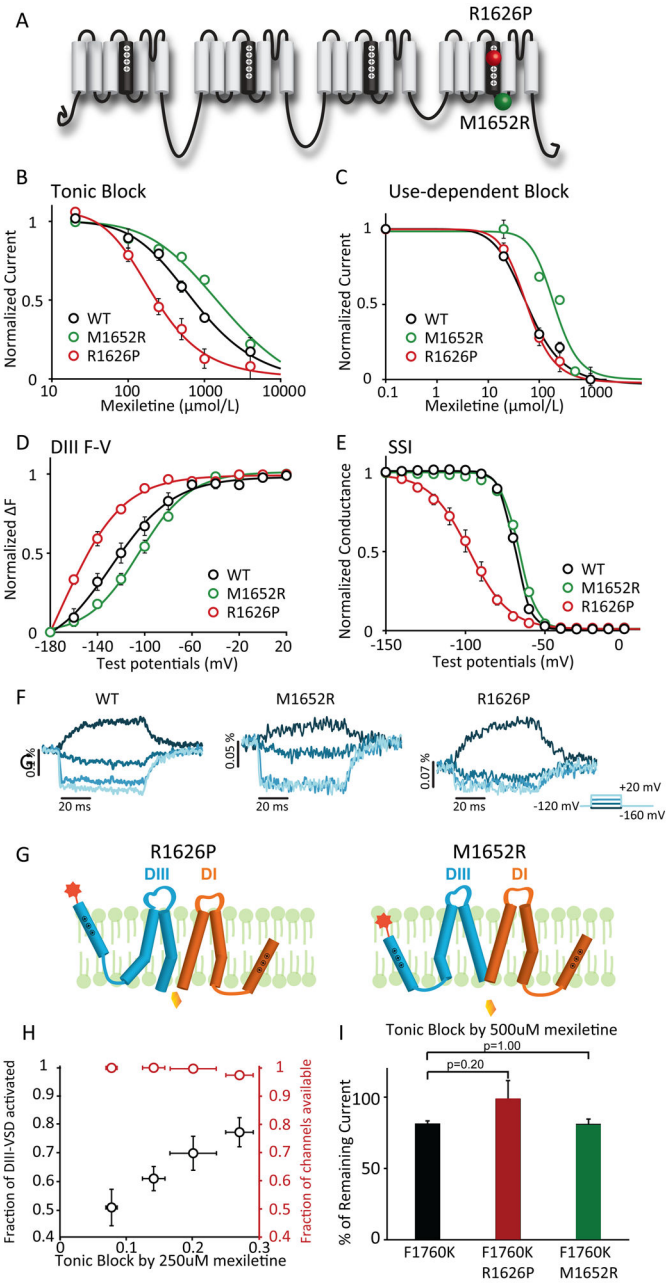

Figure 2: LQT variants with different sensitivities to mexiletine have distinct voltage dependence of DIII-VSD activation.

A. Topology of $Na_v1.5$ channel and location of the two LQT mutations with distinct mexiletine sensitivity, R1626P (red ball, sensitive) and M1652R (green ball, insensitive).

B. Concentration dependence of tonic block (TB) by mexiletine for WT, R1626P, and M1652R channels expressed in *Xenopus* oocytes (n=3 tested for each drug condition). EC_{50} values were 761 μM for WT, 2035 μM for M1652R, and 211 μM for R1626P channels.

C. Concentration dependence of use-dependent block (UDB) by mexiletine (n=3 tested for each drug condition). Currents were normalized to the peak current elicited by the first

depolarizing pulse. EC_{50} values were 58 μM for WT, 193 μM for M1652R, and 57 μM for R1626P channels.

D. Voltage dependence of steady-state fluorescence of DIII. The mean ± SEM is reported for groups of 3 to 4 cells. DIII F-V curve of M1652R showed depolarizing shift, while R1626P showed hyperpolarizing shift compared to WT channels.

E. Steady-state inactivation (SSI) curves of WT, R1626P, and M1652R channels (n=3 tested for each variant).

F. Representative DIII fluorescence traces from WT-M1296C, M1652R-M1296C, and R1626P-M1296C. All three constructs exhibit distinct fluorescence kinetics and voltage-dependence.

G. Proposed schematic showing possible mechanisms underlying the difference in mexiletine sensitivities between R1626P and M1652R. The DIII-VSD in the upward position represents the activated conformation. The lower position represents the inactivated conformation. At resting potential, R1626P has more activated DIII-VSD, which is coupled to the DIII pore domain (S5, S6), causing the pore to remain in a conformation with increase accessibility for mexiletine. In contrast, insensitive M1652R fewer activated DIII-VSDs, causing the DIII-pore to enter a conformation with less accessibility.

H. The relationships between % of block and the fraction of DIII-VSD activated, or the fraction of current available for four different holding potentials (−120, −110, −100, −90 mV) (n=3 tested for each holding potential). The fraction of current availability for four potentials are not significantly different from each other. The fraction of the DIII-VSD activated shows a linear relationship with the % of TB.

I. TB by 500 μM mexiletine for F1760K, R1626P F1760K, M1652R F1760K channels (n=4 tested for each variant). TBs are not significantly different examined with Mann-Whitney U test, suggesting that the F1760K eliminates LQT variant-dependent mexiletine sensitivity.

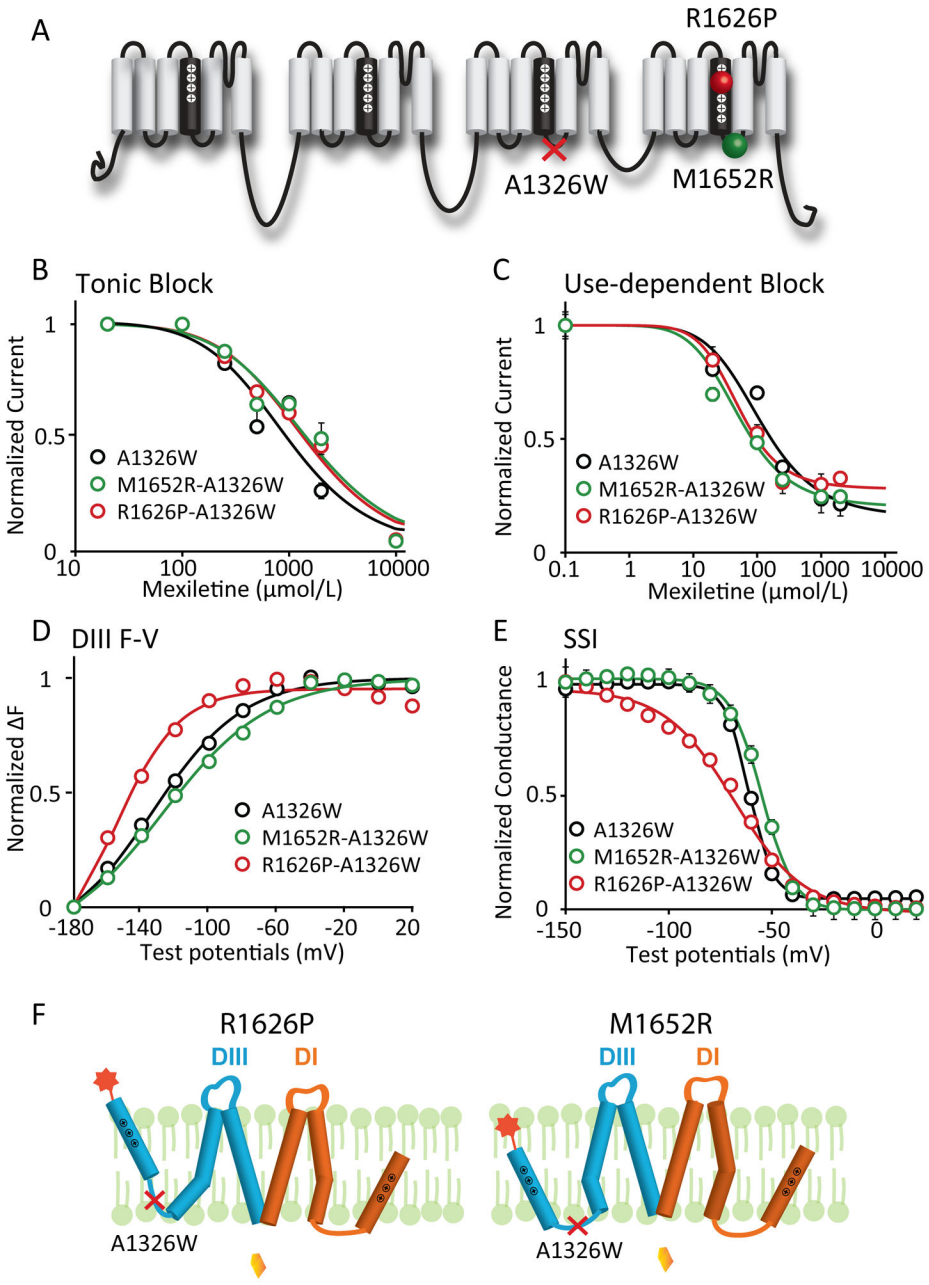

Figure 3: Mutation that decouples the DIII-VSD from DIII-pore eliminates differences in mexiletine sensitivity among LQT3 variants.

A. Locations of the decoupling mutation A1326W and two LQT3 variant mutations, R1626P and M1652R. A1326W resides on the S4-S5 linker of DIII, a motif that is known to regulate energetic coupling between the VSD and pore.

B. Concentration dependence of TB for A1326W, M1652R-A1326W, and R1626P-A1326W channels (n=3 for each drug condition). EC_{50} values were 965 μM for WT, 1562 μM for M1652R, and 1441 μM for R1626P channels.

C. Concentration dependence of UDB for M1652R-A1326W, and R1626P-A1326W channels (n=3 tested for each drug condition). EC_{50} values were 113 μM for WT, 51 μM for M1652R, and 52 μM for R1626P channels.

D. Voltage dependence of steady-state fluorescence of DIII for A1326W, M1652R-A1326W, and R1626P-A1326W channels (n=4 tested for each variant). The differences in voltage dependence of DIII-VSD activation is similar with the A1326W as a background mutation. DIII F-V curve of M1652R-A1326W still showed depolarizing shift, while R1626P-A1326W showed hyperpolarizing shift compared to A1326W channels.

E. Steady-state inactivation (SSI) curves of WT, R1626P, and M1652R channels (n=4 tested for each variant). The differences in SSI among different mutations are also preserved in presence of the A1326W background mutation.

F. Proposed schematic showing a model of how A1326W eliminates the different sensitivities among LQT variants.

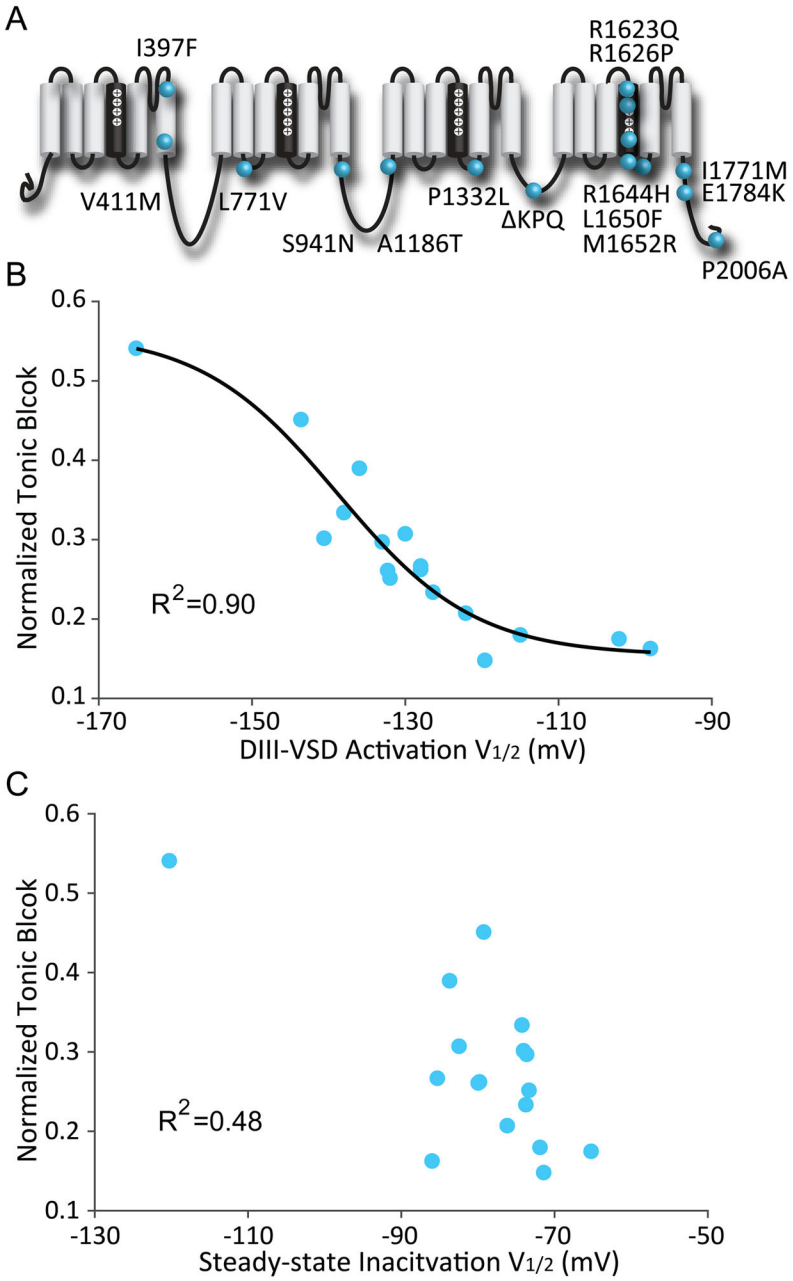

Figure 4: Voltage dependence of DIII-VSD activation strongly correlates with tonic block by mexiletine.

A. Locations along the primary sequence and channel topology of 15 LQT3 variants tested.

B. Relationship between the voltage dependence of DIII-VSD activation ($V_{1/2}$ of DIII F-V) and normalized tonic block by mexiletine. The mean ± SEM is reported for groups of 3 to 4 cells. The data were fitted with a Boltzmann function and the correlation calculated. A strong correlation (R^2=0.9) between these two parameters were observed when fitted with a Boltzmann function.

C. Relationship between the SSI ($V_{1/2}$ of SSI) and normalized tonic block by mexiletine. The mean ± SEM is reported for groups of 3 to 4 cells. The two parameters are not well-

correlated, suggesting that channel inactivation is not a good predictor of mexiletine tonic block.

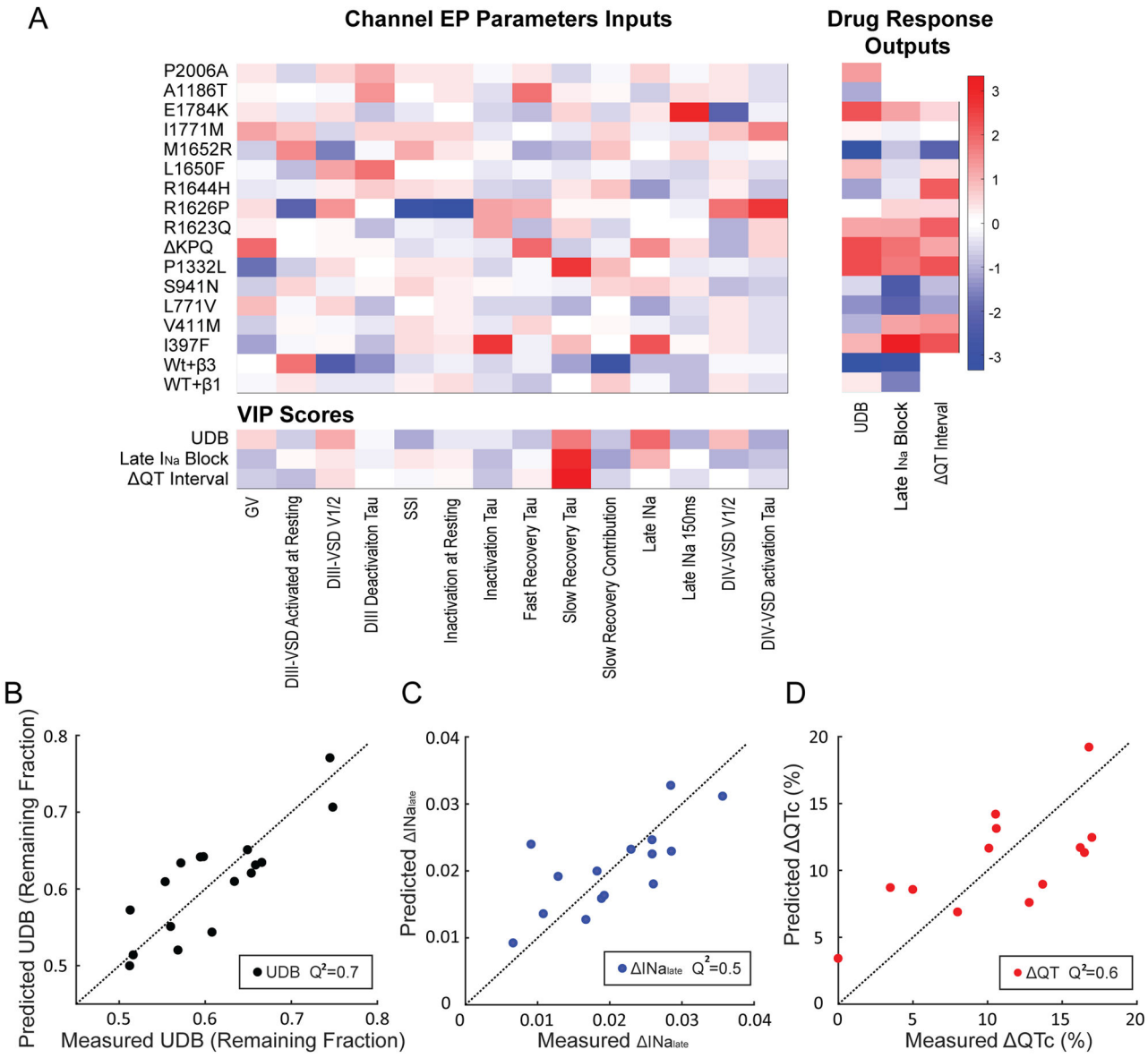

Figure 5: Partial least square (PLS) regression model can predict UDB and QT_c shortening by mexiletine from channel gating parameters.

A. Left: heatmap of 14 quantified electrophysiological parameters (EP) of the gating for 15 LQT3 variants and WT channels with β1 or β3 subunits. Right: heatmap of each channel's responses to mexiletine, including UDB, late I_{Na} block and QT_c shortening (ΔQT_c) in LQT3 patients undergoing mexiletine treatment. EP parameters and mexiletine blockade were reported as the mean for groups of 3-4 cells. Bottom: VIP scores for each gating parameter. VIP scores were ranked by each parameter's impact on model fitness. Each gating parameter is removed individually, and PLSR model was constructed with the rest of parameters. The corresponding model fitness was calculated based on Q^2 of measured block and predicted block with leave-one-out cross-validation. Higher VIP score (red) suggests that the gating parameter is more important for improving the model fitness.

B-D. Relationship between measured and predicted UDB, late I_{Na} block or ΔQT_c. The predictions were made using the PLS regression model with selected parameters with high VIP scores. Model stability was tested with leave-one-out cross validation.

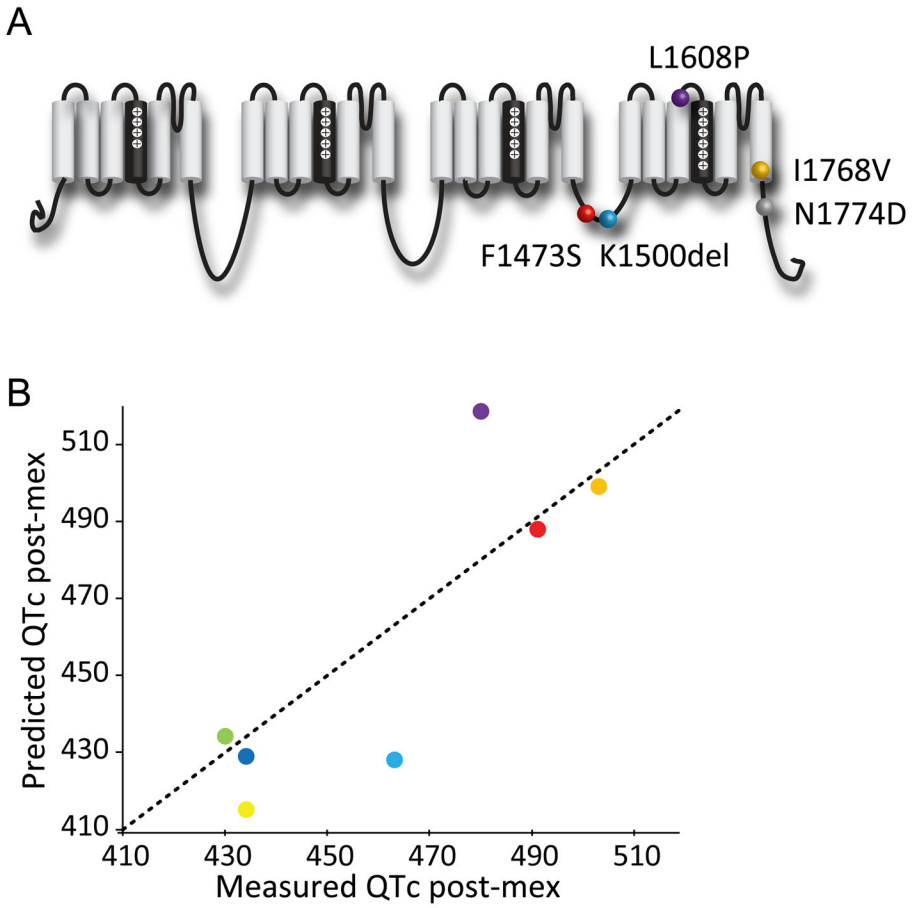

Figure 6: PLS regression model predicts QT_c shortening by mexiletine for genetic variants

A. Locations of 5 LQT3 variants that are included in the clinical trial and were not used for training the model.

B. Comparison of the measured patients' QT_c after mexiletine therapy and the predicted QT_c after mexiletine using the PLS regression model.

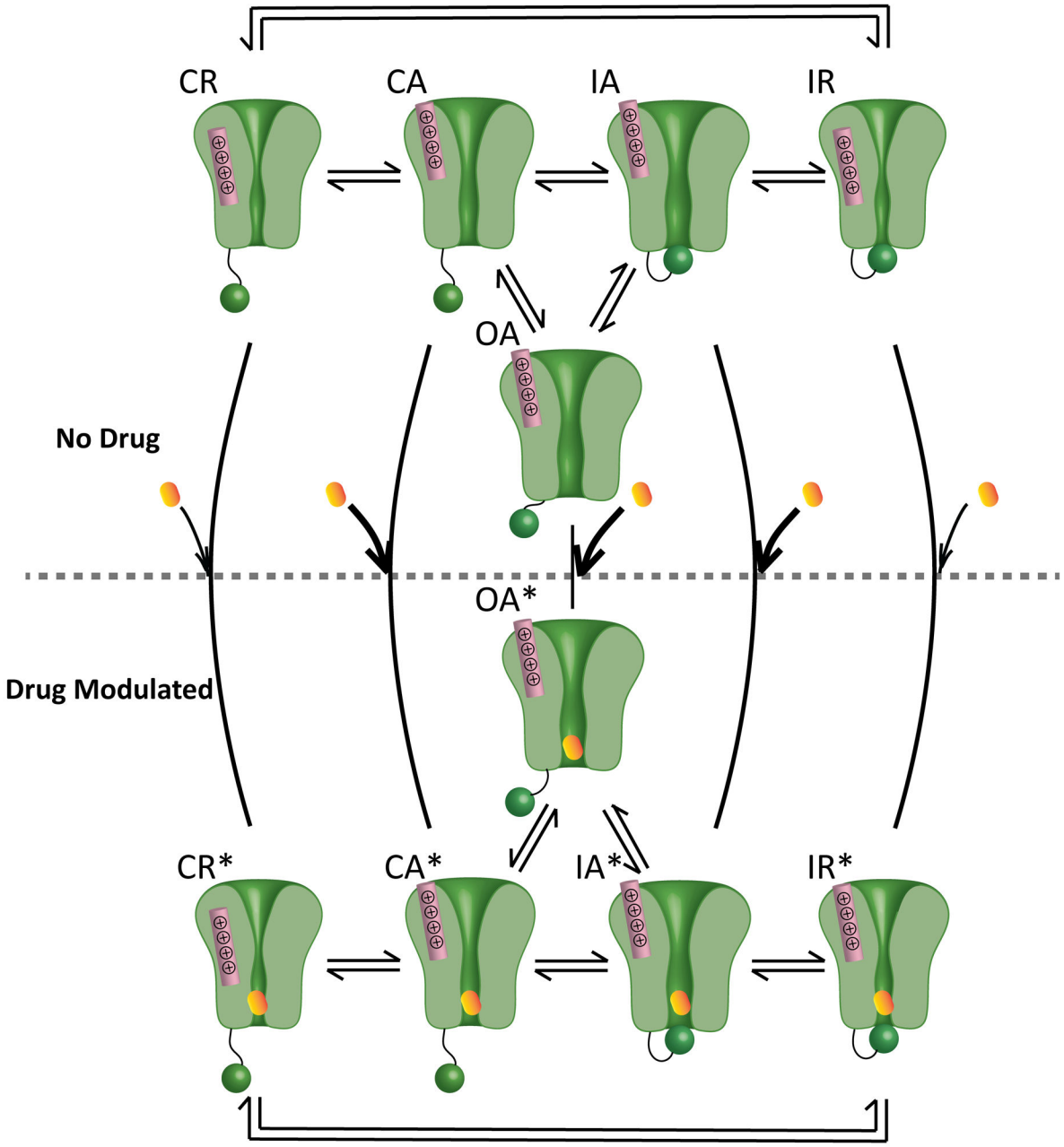

Figure 7: Proposed updated VSD-modulated receptor model for Class Ib antiarrhythmics.

The model comprises five states, CR, CA, OA, IA, and IR. R and A represent the DIII-VSD at resting and activated positions, respectively. C, O, and I represent closed, open and inactivated states of the pore. Mexiletine has different binding affinity to each state. Thick arrows represent high binding affinity, and the thin black arrows represent low binding affinity. After mexiletine blocks the pore, channels enter five drug modulated states, CR*, CA*, OA*, IA*, and IR*. The transition rates between modulated states change compared to those between the unmodulated states. This model provides a molecular basis for how mexiletine preferentially blocks the channel when the DIII-VSD is activated (CA, OA, IA).

Table 1:

Mexiletine QT_c trial outcomes.

7 out of 8 patients have clinical measured QT_c post mexiletine that fall into the predicted range.

Genetic Variants	baseline QT_c	Measured post mex QT_c	Predicted post mex QT_c	Prediction lower bound	Prediction upper bound
F1473S	550	491	488	449	526
I1768V	520	503	499	462	520
K1500del	478	434	415	381	449
K1500del	500	430	434	399	469
K1500del	493	463	428	393	463
K1500del	494	434	429	394	463
L1608P	604	480	518	477	558
N1774D	814	610	750	693	807